Evaluation of the NCEP/NCAR reanalysis in the NE Pacific and the Bering Sea

Carol Ladd

Pacific Marine Environmental Laboratory, National Oceanic and Atmospheric Administration (NOAA), Seattle, Washington, USA

Nicholas A. Bond

Joint Institute for the Study of the Atmosphere and Ocean, University of Washington, Seattle, Washington, USA

Received 27 September 2001; revised 3 July 2002; accepted 26 July 2002; published 18 October 2002.

[1] The quality of the National Center for Environmental Prediction (NCEP)/National Center for Atmospheric Research (NCAR) reanalysis surface forcing fields is evaluated for the Bering Sea and the NE Pacific using a series of buoy measurements from 1995 to 2000. Because the mooring data have not been assimilated into the reanalysis, they provide an independent measure of the accuracy of the reanalysis in these regions. Emphasis is placed on 10 m winds and shortwave radiation, as they are important parameters for forcing ocean models. Except close to the coast where the reanalysis does not adequately account for the blocking influence of the topography, wind directions were accurately estimated by the reanalysis. Comparisons with the reanalysis suggest a small bias with NCEP 10 m winds greater than observed by ~5%. In the Bering Sea, downward shortwave radiation in the reanalysis is overestimated by roughly 70–80 W m^{-2} averaged over the summer data. In the NE Pacific, the reanalysis overestimates downward shortwave radiation by approximately 20 W m^{-2} in both summer and winter. Inaccurate representation of clouds in the reanalysis model is the most likely reason for the overestimate. Analysis of weather patterns during periods of particularly large overestimation of shortwave radiation suggests that the reanalysis better reproduces cloudiness during synoptic-scale cyclonic disturbances and is less able to accurately reproduce low clouds and sea fog in fair weather conditions. *INDEX TERMS:* 3337 Meteorology and Atmospheric Dynamics: Numerical modeling and data assimilation; 3359 Meteorology and Atmospheric Dynamics: Radiative processes; 4504 Oceanography: Physical: Air/sea interactions (0312); *KEYWORDS:* shortwave radiation, winds, NCEP, Bering Sea

Citation: Ladd, C., and N. A. Bond, Evaluation of the NCEP/NCAR reanalysis in the NE Pacific and the Bering Sea, *J. Geophys. Res.*, *107*(C10), 3158, doi:10.1029/2001JC001157, 2002.

1. Introduction

[2] Scarcity of atmospheric forcing data has always been a limiting factor in oceanographic research. Many studies have addressed this limitation by using a data set based on hindcasts from a global numerical weather prediction model constrained by continuous assimilation of available observations. One of the most widely used is the National Center for Environmental Prediction (NCEP)/National Center for Atmospheric Research (NCAR) reanalysis project (hereafter NCEPR), a global data set of oceanographic and atmospheric parameters created with a temporally consistent framework [*Kalnay et al.*, 1996; *Kistler et al.*, 2001]. Output from the NCEPR has been used in studies of air–sea interaction in the Bering Sea and NE Pacific [e.g., *Flatau et al.*, 2000; *Bond and Adams*, 2002; *Hermann et al.*, 2002] in addition to other regional and global studies.

0148-0227/02/2001JC001157$09.00

[3] Many studies have evaluated the quality of the NCEPR in the tropics [e.g., *Bony et al.*, 1997; *Shinoda et al.*, 1999; *Wang and McPhaden*, 2001] or globally [e.g., *Weare*, 1997; *Scott and Alexander*, 1999; *Yang et al.*, 1999] but no systematic evaluations have been produced for the Bering Sea and the NE Pacific. The SE Bering Sea shelf and the NE subarctic Pacific are important regions ecologically and economically, producing approximately half of the United States fishery production [*National Research Council Committee on the Bering Sea Ecosystem*, 1996]. Due to inhospitable weather and remote location, however, little historical data is available in this region. In 1984, the National Oceanic and Atmospheric Administration (NOAA) established the Fisheries Oceanography Coordinated Investigations (FOCI) program to study the influence of the physical environment on the abundance of various commercially valuable fish and shellfish stocks in these regions. This program has compiled a database of observations from moorings in the Bering Sea that can be used to evaluate the quality of reanalysis output in this region. In addition, data collected at the OWS Papa

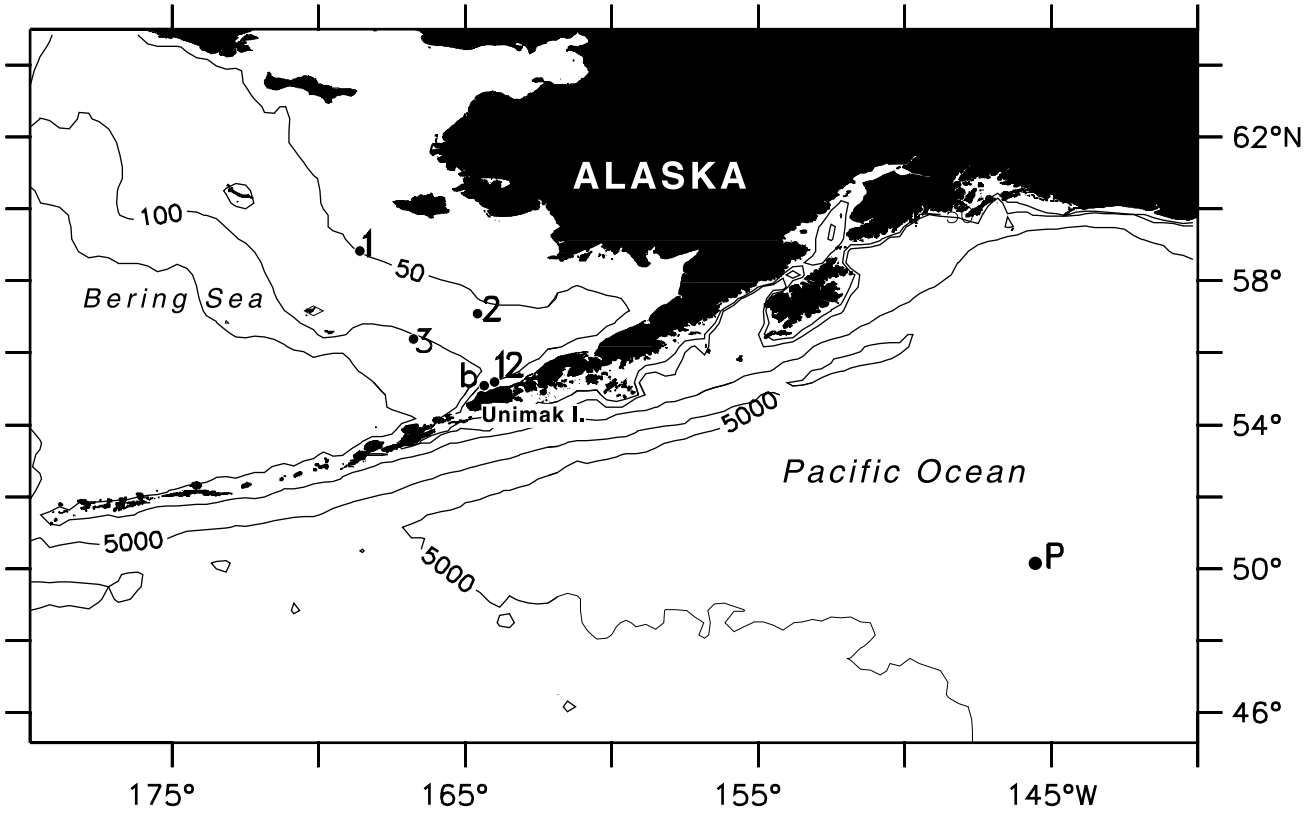

Figure 1. Map of Bering Sea and NE Pacific. Numbers and letters denote location of moorings. Contours indicate bathymetry.

location provide a comparison between the Bering Sea and the NE Pacific. Because the mooring data have not been assimilated into NCEPR, they provide an independent measure of the accuracy of NCEPR in these regions.

[4] This paper is organized as follows. Meteorological buoy data is described in section 2. The NCEPR is described in section 3. Evaluations of winds and shortwave radiation are presented in sections 4 and 5, respectively. Section 6 presents a summary and discussion.

2. Data

[5] The data used in this comparison were collected over a series of years by moored buoys in the Bering Sea and the NE Pacific (Figure 1 and Table 1). The surface buoys were 2.3 m diameter fiberglass toroids connected by chain to a tether and anchored to the bottom. The surface toroids had a tower, approximately 3 m tall, on which was mounted a pyranometer to measure solar radiation from ~0.3 to 2.8 μm (either Eppley Precision Spectral or LI-COR LI-200SA), R.M. Young model 05103 wind sensors, Rotronics model MP100 air temperature/relative humidity sensors, and Yellow Springs Instruments thermistors to measure sea surface temperatures. All sensors were calibrated in our laboratory or by the manufacturer a few months prior to and after use. Additional details about these moorings can be found in the work of *Stabeno et al.* [1998].

3. NCEP/NCAR Reanalysis

[6] We compare the data described in the preceding section with output from the NCEP/NCAR Reanalysis data set [*Kalnay et al.*, 1996; *Kistler et al.*, 2001]. The NCEPR is an ambitious project designed to provide a long-term (more than 50 years) record of atmospheric variables to support the climate research and monitoring communities. The data assimilation system is kept unchanged over the reanalysis period to eliminate any perceived climate shifts due to changes in the assimilation system. The NCEPR continues to be updated with current data and gridded output can be downloaded from the NOAA-CIRES Climate Diagnostics Center Web site at http://www.cdc.noaa.gov/.

Table 1. Data Used in Comparison

Name	Latitude	Longitude	SW radiation?	Dates
Mooring 1	58.7°N	168.3°W	No	June–September 1997, April–September 1998
Mooring 1b	55.1°N	164.5°W	No	March–June 1995
Mooring 2	56.9°N	164.1°W	1996, 1999	April–September 1996, 1997, 1999, 2000
Mooring 3	56.1°N	166.3°W	1995, 1996, 1997	May–August 1995, April–September 1996, April–August 1997
Mooring 12	55.3°N	164.0°W	No	April–September 1999
Papa	50°N	145°W	1998/1999, 1999/2000	October–February 1998/1999, October–March and June–July 1999/2000

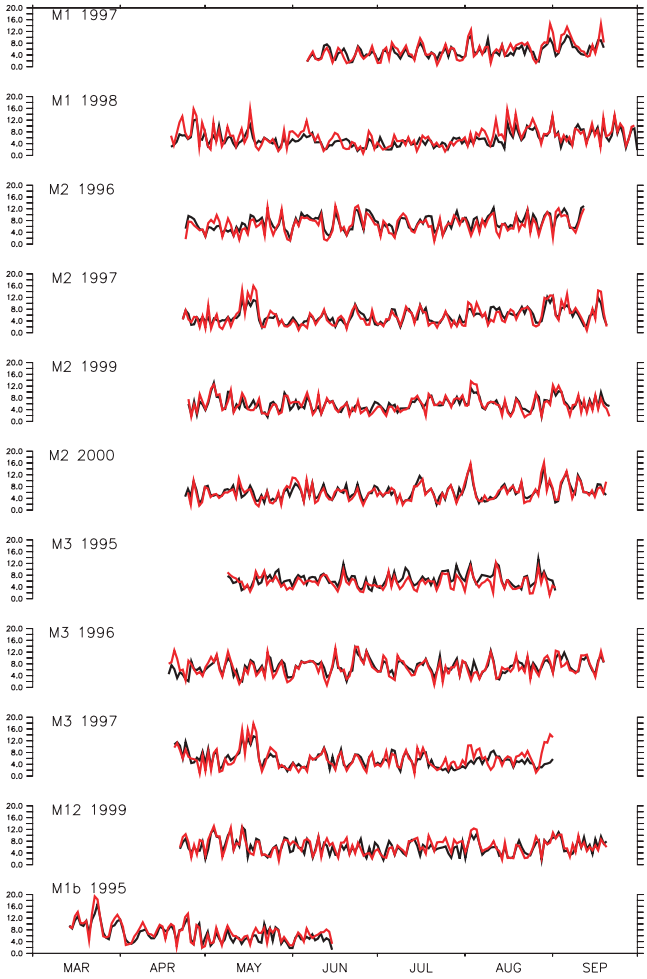

Figure 2. Time series of wind speed from the Bering Sea mooring deployments (black) and from the NCEPR (red).

[7] The project involves collection, quality control, and assimilation of land surface, ship, rawinsonde, pibal, aircraft, satellite, and other data. The data assimilation system includes the NCEP T62 global spectral model with 28 vertical levels. The T62 resolution is equivalent to about 210 km horizontally [*Kalnay et al.*, 1996].

[8] The NCEPR gridded fields have been classified into three categories, depending on the relative influence of the observational data and the model on the gridded variable. Winds and upper-air temperatures are classified as *type A* variables indicating that they are strongly influenced by data and are the most reliable. Surface air temperatures and relative humidity represent *type B* variables since they are influenced both by the observations and by the model, and are therefore less reliable. Heat fluxes at the surface are classified as *type C* variables indicating that they are derived solely from the model fields and are the least reliable [*Kalnay et al.*, 1996].

[9] The reanalysis output used in this comparison consists of gridded daily (shortwave radiation) and 6 hourly (winds) averages on a Gaussian grid (~1.9° grid spacing). To facilitate comparison, except in the case of Mooring 1b and Mooring 12, the NCEPR parameters were linearly interpolated to the location of the moorings. For those two moorings, the surrounding four NCEPR grid points include points in the North Pacific south of the Aleutian Islands that may be governed by different dynamics. Thus the data were compared to the NCEPR at the single nearest grid point instead of an interpolation between the four surrounding grid points.

4. Winds

[10] Wind data were obtained from all of the moorings listed in Table 1. Prior to any analysis, wind speed (Figures 2 and 3) and the zonal and meridional components of the wind data were adjusted to 10 m height assuming neutral stability and a logarithmic wind profile [*Large and Pond*, 1981] and averaged over 6 hour intervals to compare to the NCEPR 6 hour averaged 10 m winds.

[11] Due to the possibility of sea ice during the winter in the Bering Sea, most of the data were taken during the summer (April–September) when winds tend to be weaker than during winter. The two exceptions are the Papa mooring, which includes winter data, and Mooring 1b, which includes March data. The maximum daily averaged wind speed for the summer data (~14.3 m s^{-1}) occurred in May 1997 at Mooring 3. This strong wind event was also observed at M2 (Figure 2). The Papa mooring recorded a maximum daily averaged wind speed of 17.7 m s^{-1} that occurred in December 1998 (Figure 3) and Mooring 1b recorded a maximum of 16.5 m s^{-1} in March 1995 (Figure 2). Wind speed averaged over the deployments was ~5.5 m s^{-1} at the Bering Sea moorings. At the Papa mooring, June–July data averaged ~6 m s^{-1} while September–February data averaged ~9 m s^{-1}.

[12] To evaluate the quality of NCEPR winds, correlations between 10 m, 6 hour averaged wind data from the moorings and from NCEPR were calculated. Correlations were calculated for zonal and meridional winds individually, and in addition, complex correlations [*Kundu*, 1976] were calculated to estimate the correlation of the vector winds and to estimate a correlation angle. The complex correlation is independent of the choice of coordinate system. The results of these analyses are summarized in Table 2.

[13] Correlations between the mooring wind data and the NCEPR winds were quite good (>0.80; significant at 99.9%) with the highest complex correlation (0.95) found for Mooring 2 data in 1996. In addition, with a few exceptions, the correlation angle is less than 10°. The wind sensor manufacturer notes an instrument accuracy of ±3°. However, *Freitag et al.* [2001] report direction error, including both compass and vane error, of 7.8°. High correlations with the

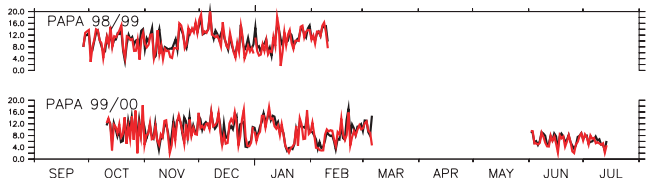

Figure 3. Time series of wind speed from the OWS Papa mooring deployments (black) and from the NCEPR (red).

Table 2. Correlations Between Wind Data From Moorings and From Reanalysis

	Year	U corr. coeff.	V corr. coeff.	Complex corr. coeff.	Complex corr. angle
Mooring 1	1997	0.88	0.86	0.83	5
	1998	0.86	0.86	0.82	−4
Mooring 2	1996	0.93	0.91	0.92	−9
	1997	0.90	0.91	0.90	2
	1999	0.91	0.87	0.89	−6
	2000	0.87	0.87	0.90	16
Mooring 3	1995	0.94	0.94	0.94	−3
	1996	0.84	0.91	0.88	−7
	1997	0.82	0.87	0.85	4
Mooring 12	1999	0.84	0.72	0.82	19
Mooring 1b	1995	0.90	0.96	0.93	2
Papa	1998/1999	0.93	0.85	0.92	−1
	1999/2000	0.86	0.86	0.90	−4

Positive (negative) correlation angle implies that reanalysis is rotated counterclockwise (clockwise) with respect to mooring data.

NCEPR are expected due to the large horizontal scales (~1000 km) of the pressure patterns producing these winds. On these scales, pressure is reasonably well sampled by the operational observing network and the resulting winds are well diagnosed by the NCEPR model/assimilation system (as discussed by *Bond and Adams* [2002]).

[14] The lowest complex correlation (0.80) and largest complex correlation angle (19°) occur at Mooring 12 in 1999 (Figure 4). The positive correlation angle indicates that the NCEPR winds are rotated 19° counterclockwise with respect to the mooring data. Average winds for the month of August 1999 (Figure 5b) show the influence of the Alaska Peninsula and Aleutian Islands on winds at Mooring 12 as compared to NCEPR. Shishaldin Volcano (elevation 2857 m) on Unimak Island is due south of Mooring 12 and only 0.5° of latitude (55.6 km) away. The internal deformation radius (over which topographic effects would be important) is,

$$l_R = \frac{ND}{f},$$

where N is the Brunt–Väisälä frequency, D is the height of the upstream topography, and f is the Coriolis parameter. Using $N = 1.2 \times 10^{-2}$ s^{-1}, the average Brunt–Väisälä frequency for the atmosphere, and $D = 2800$ m, Shishaldin Volcano can be expected to influence the winds within roughly 280 km.

[15] Given the T62 resolution, the NCEPR cannot adequately resolve the effects of topography this close to the coast. In contrast, the winds at Mooring 2 during the same time period were much more strongly aligned with the NCEPR winds (Figure 5b). The correlation coefficient between mooring 12 data and NCEPR winds is lower for the meridional component (0.70) than for the zonal component (0.82). This is not surprising as the coastline is oriented roughly zonally and would be expected to primarily influence the meridional component of the wind. Rotating the coordinate system into along-shore and cross-shore directions, results in correlation coefficients of 0.66 (cross-shore) and 0.83 (along-shore).

[16] Coastal winds generally tend to be aligned with topography [e.g., *Dorman and Winant*, 1995; *Bond and Stabeno*, 1998; *Stanton*, 1998]. Interestingly, the principal axis (axis of maximum variance) of Mooring 12 winds is rotated ~60° with respect to the along-shore direction. The principal axis of Mooring 12 winds is 304° while the principal axis of NCEPR winds at the closest grid point (165°W, 55°N) is 313°. The coastline orientation is ~65/245°. These winds are not very strongly polarized with the principal axis accounting for ~65% of the variance. The large amount of scatter in the wind direction at Mooring 12 is presumably due to the combination of the weather variability of the region and the mesoscale structure in the terrain comprising the Aleutian chain.

[17] The RMS difference between the meridional components of Mooring 12 and NCEPR winds is dependent on wind direction. When winds are southerly at Mooring 12, the RMS difference is 4.4 m s^{-1}, while during northerly winds the RMS difference is 2.6 m s^{-1}. In addition, NCEPR tends to overestimate speeds (Figure 4) during southerly winds, indicating that it does not adequately account for the blocking influence of the topography.

[18] Mooring 1b in 1995 was very close to the Mooring 12 location (Figure 5a and Table 1) and would be expected to show the same topographic influence. However, because winds were primarily northerly and westerly during the Mooring 1b deployment, the wind direction at Mooring 1b is closely aligned with the NCEP wind direction. This result indicates that care must be taken when using NCEPR winds particularly close to the coast.

[19] Excluding Moorings 1b and 12 (because of the topographic influence discussed above), the NCEPR overestimates wind speeds by ~5% at the Bering Sea and Papa moorings with an RMS difference of 1.9 m s^{-1}. This is in contrast to a comparison of NCEPR winds with high-quality research vessel observations that showed that the NCEPR generally underestimates near-surface wind speed at all

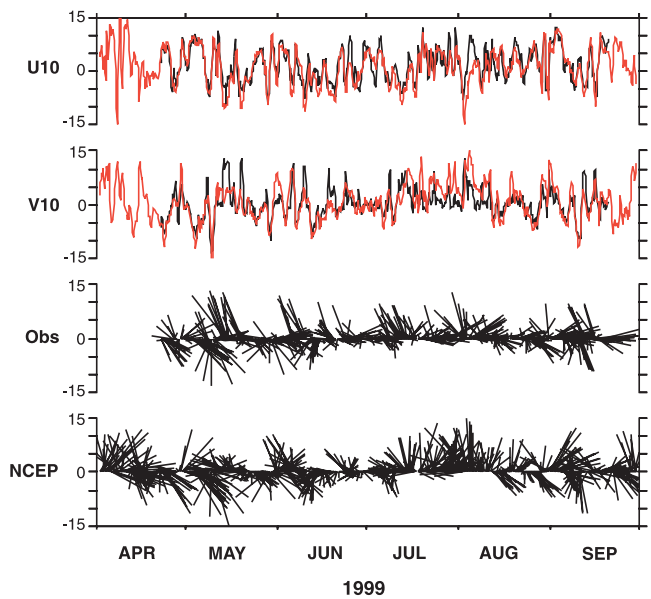

Figure 4. Zonal (U) and meridional (V) wind components, observed wind vectors, and NCEPR wind vectors (m s^{-1}) from Mooring 12 location.

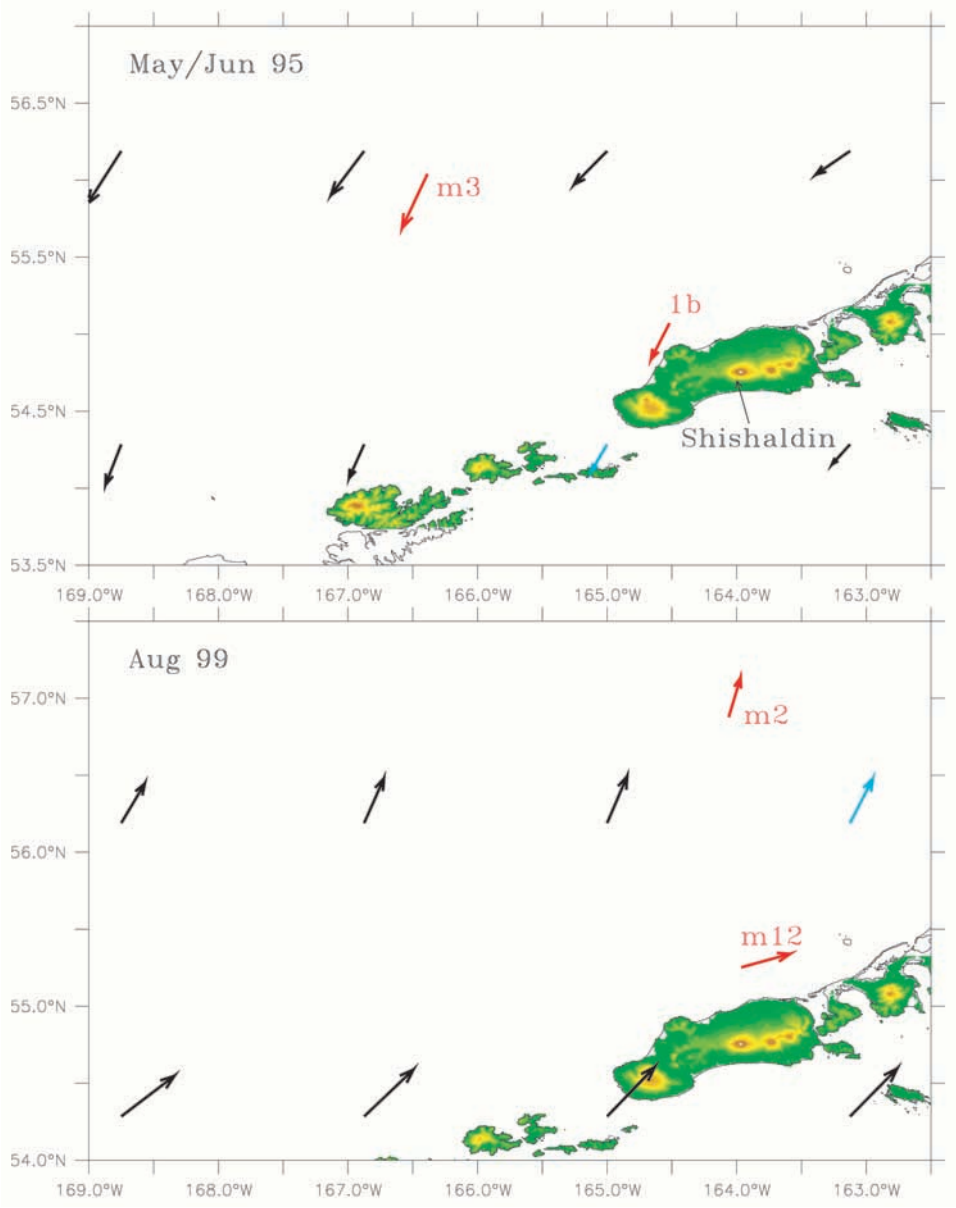

Figure 5. NCEPR and mooring winds averaged over (a) May–June 1995 and (b) August 1999. The topography of Unimak Island (and other Aleutian Islands) is denoted in color with an arrow denoting Shishaldin Volcano. The red vectors denote average mooring winds while the black vectors denote NCEPR winds. The blue vectors denote wind at the nearest NCEPR grid point to Mooring 1b (a) and Mooring 12 (b).

latitudes [*Smith et al.*, 2001] although very little of their data came from the Bering Sea.

5. Surface Shortwave Radiation

[20] Shortwave radiative transfer processes in NCEPR are calculated using parameterizations developed by *Lacis and Hansen* [1974]. The reanalysis model considers surface albedo and absorption by ozone, carbon dioxide, water vapor, and clouds in the calculation of the shortwave radiation [*Kanamitsu*, 1989].

[21] *Bony et al.* [1997] compare radiation parameters calculated by the reanalysis created by the Data Assimilation Office (DAO) of Goddard Laboratory for Atmospheres with those from the NCEP reanalysis. In the tropics the DAO and NCEP reanalyses produce surface net heat fluxes that can differ by up to 50 W m^{-2} in the average and by a factor of 2 when considering interannual anomalies. Thus, they note the importance of evaluating reanalysis surface heat fluxes before using them to force ocean models.

[22] *Hermann et al.* [2002] force a regional model of the Bering Sea with surface heat flux fields from the NCEP reanalysis. They find that the modeled water column begins to stratify earlier, and heats up more in the spring and summer, than is observed in the data. They suggest that this may be due to an overestimate of surface heat flux from the

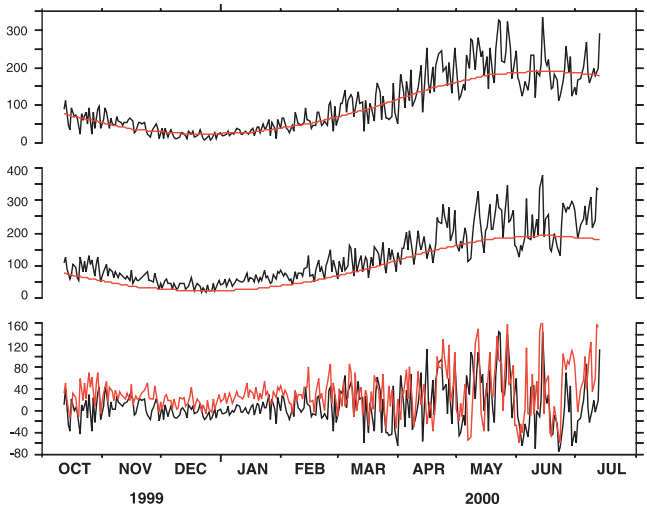

Figure 6. Shortwave radiation fluxes (W m^{-2}). (a) From the Papa mooring in the winter of 1999–2000 (black). Seasonal cycle from ASMD (red). (b) From the NCEP/NCAR reanalysis (black). Seasonal cycle from ASMD (red). (c) Anomalies from the ASMD seasonal cycle. Papa mooring data (black) and reanalysis data (red).

NCEP data. Thus an evaluation of the quality of NCEPR shortwave radiation will be useful in future regional studies.

[23] To evaluate the shortwave radiation fluxes in the NCEP reanalysis, we compare daily average surface downward solar radiation flux from the NCEPR with downward solar radiation measurements (Q_i) from two of the Bering Sea mooring locations (2 and 3) and the Papa moorings in the NE Pacific over multiple years (Table 1). A seasonal cycle was removed from both the mooring data and NCEPR prior to calculating correlations. Because the mooring deployments were of limited duration, the mooring data could not be used to calculate a seasonal cycle. Thus, the seasonal cycle was calculated from the Atlas of Surface Marine Data 1994 (ASMD) [*da Silva et al.*, 1994] monthly surface shortwave radiation climatology by linearly interpolating to daily values and to the location of the moorings. The ASMD is based on the Comprehensive Ocean–Atmosphere Data Set (COADS) and represents the seasonal cycle of shortwave fluxes adequately for our purposes (Figure 6). After removing the seasonal cycle, correlations between Q_i from the moorings and from NCEPR (Figures 7 and 8) were significant at a 95% confidence level (assuming an autocorrelation timescale of 5 days) for all of the deployments except Mooring 3 in 1995 (Table 3).

[24] Since shortwave radiation is classified as a C variable, it is no surprise that the shortwave correlations are much lower than the wind correlations. The highest Q_i correlations are found during the winter at the Papa mooring. Correlation coefficients for both years for winter data (October–February) only at the Papa mooring are greater than 0.6. During the summer of 2000, NCEPR is correlated with the Papa data with a correlation coefficient of only 0.43.

[25] Of the data considered here, correlations are the weakest at Mooring 3. The percentage of cloud cover is high (>80% during summer; Figure 9) over the Bering Sea and would be expected to have large impacts on incoming shortwave radiation in this region. *Scott and Alexander* [1999] compare net surface shortwave fluxes from the NCEP reanalysis with those from the European Center for Medium-Range Weather Forecasts reanalysis and with National Aeronautics and Space Administration/Langley satellite data. They find that both reanalyses have a positive bias where low-level stratiform clouds are most common (as in the Bering Sea during summer [*Norris*, 1998]) and a negative bias where cumuliform clouds are dominant. According to data from the International Satellite Cloud Climatology Project (ISCCP) [*Rossow and Schiffer*, 1991], the Mooring 3 location is slightly cloudier and has a higher percentage of low clouds than the Mooring 2 location. We speculate that errors in the NCEPR clouds may contribute to the lower correlations at Mooring 3. The influence of clouds is further discussed below.

[26] Biases, calculated as the difference between the NCEPR and mooring shortwave radiation, averaged over each mooring deployment are shown in Table 3. As suggested by *Hermann et al.* [2002], NCEPR overestimates Q_i. In the Bering Sea, Q_i is overestimated by roughly 70–80 W m^{-2} averaged over the summer data except at Mooring 3 in 1995 when the bias was 94 W m^{-2} (Figure 7). In the NE Pacific (Papa), the overestimate is smaller: approximately 20 W m^{-2} (Figure 8). The Papa data are primarily from the winter when incoming shortwave radiation is much smaller than during the summer. However, the bias is on the order of 20 W m^{-2} even for the April–September Papa data alone.

[27] The difference in bias between the Papa location and the Bering Sea data could be due to differences in clouds or sea fog. While stratus cloudiness is dominant in both regions, sky-obscuring fog, a component of stratus cloudi-

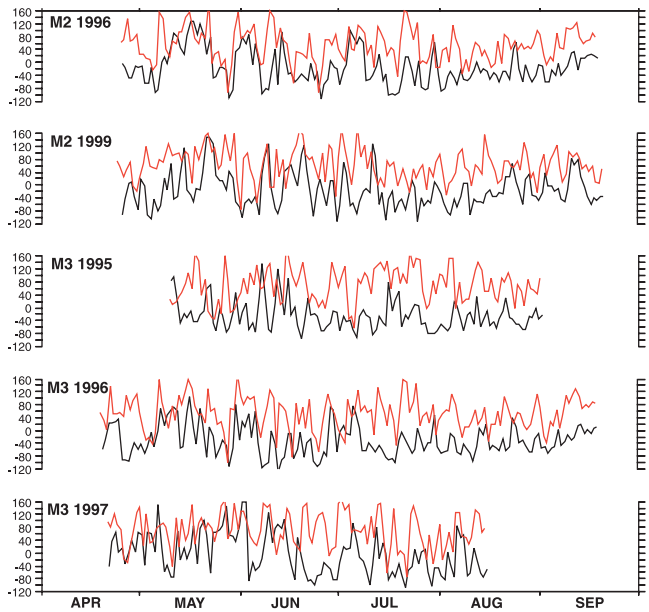

Figure 7. Shortwave radiation flux anomalies from the ASMD seasonal cycle (W m^{-2}) from the Bering Sea mooring deployments (black) and from the NCEPR (red).

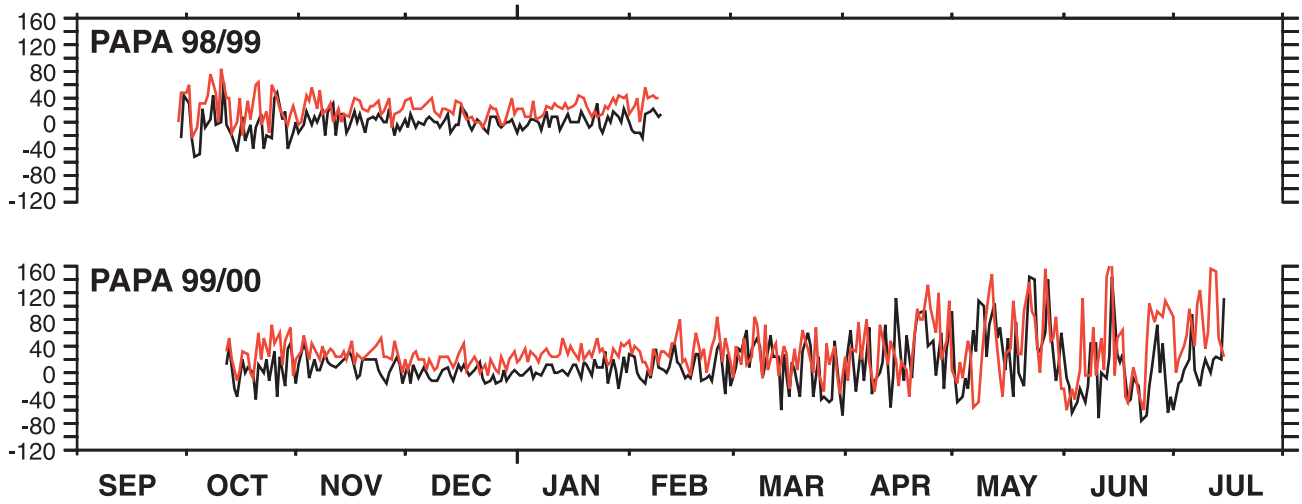

Figure 8. Shortwave radiation flux anomalies from the ASMD seasonal cycle (W m^{-2}) from the Papa mooring deployments (black) and from the NCEPR (red).

ness, is more common in the Bering Sea than at Papa [*Klein and Hartmann*, 1993] and is probably not parameterized well by NCEPR.

[28] At both Mooring 2 and Mooring 3, amplitude, and variability are damped in July–September compared to earlier in the spring and summer (Figure 7a). For example, at Mooring 3, July–September shortwave radiation (averaged over all three years with seasonal cycle removed) is ~20 W m^{-2} less and the variance is reduced to less than half of that in April–June. A weaker damping is also present in NCEPR (July–September mean shortwave radiation is smaller by ~3 W m^{-2} and variance is reduced ~10% compared with April–June). This situation results in NCEPR underestimating variability in April–June and overestimating it in July–September. The reduction in magnitude and variability of Q_i late in the summer could be due to two factors:

1. Low stratus clouds are common in the North Pacific and Bering Sea [*Norris*, 1998]. According to ISCCP data, cloudiness in the Bering Sea is greatest in June–September and a large part of that is low stratus. NCEPR climatological total cloud cover is consistently smaller than that from the ISCCP data (Figure 9). The largest difference between the two data sets occurs June–September. Thus, NCEPR is probably underestimating cloudiness in the Bering Sea, particularly during the late summer.

2. It is possible that the measurement at the mooring is degraded late in its deployment due to salt accumulation on the sensor. However, the fact that the damping is represented by NCEPR data, although weaker than in the mooring data, suggests that it is probably due to mechanisms such as clouds present in the reanalysis model but not of adequate strength.

[29] In order to evaluate under what conditions the NCEPR more accurately estimates Q_i, the mean and standard deviation of the difference between NCEPR and Mooring Q_i were calculated. Differences between NCEPR and Mooring Q_i were negatively correlated with NCEPR net shortwave cloud forcing suggesting that inaccuracies in NCEPR clouds are at least partially responsible for inaccuracies in Q_i. The sign of the correlation (increased (NCEPR − Mooring Q_i) associated with decreased NCEPR cloud forcing) implies that NCEPR overestimates Q_i more during periods when NCEPR cloud forcing of shortwave radiation is weak. Wind patterns (from NCEPR) during days when the difference exceeded the mean plus one standard deviation (NCEPR highly overestimating Q_i) were examined and compared with days when the difference was less than the mean minus one standard deviation (NCEPR more accurately estimating Q_i). For each summer, there were approximately 25 days in each category. Out of the 70 total days (during

Table 3. Correlations Between Downward Shortwave Radiation Data From Moorings and From Reanalysis (Seasonal Cycle Removed)

	Year	Correlation coeff.	Bias (W m^{-2})	Notes
Mooring 2	1996	0.59	68	
	1999	0.49	77	
Mooring 3	1995	0.12	94	Not significant
	1996	0.36	83	
	1997	0.39	72	
Papa	1998/1999	0.65	22	October–February only
	1999/2000	0.49	22	October–February: corr. = 0.62 April–July: corr. = 0.43

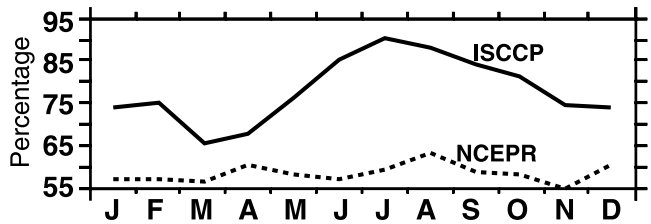

Figure 9. Monthly climatology of cloud cover averaged over the eastern Bering Sea (55.5–58°N, 170–163°W), from the ISCCP (solid) and from the NCEPR (dash).

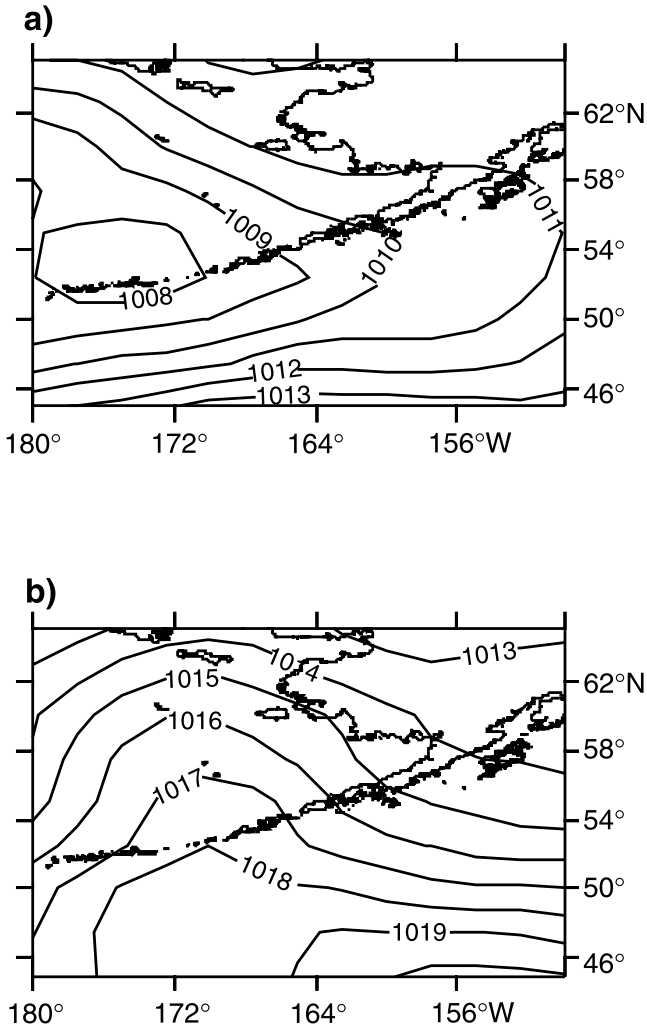

Figure 10. Sea level pressure (mbar) composites calculated from the NCEPR. (a) Averaged over 24 days in 1997 when the NCEPR most closely represents the mooring Q_i. (b) Averaged over 23 days when the NCEPR most overestimates Q_i.

1996, 1997, and 1999) when NCEPR Q_i was highly overestimated, about 35% exhibited northwesterly winds over the SE Bering Sea, as opposed to only 18% when the NCEPR more accurately estimated Q_i. In contrast, southerly winds were exhibited 21% of the time when NCEPR Q_i was highly overestimated and 45% of the time when NCEPR more accurately estimated Q_i. Often, these southerly winds were associated with approaching cyclones, which were much less frequent during periods when the NCEPR highly overestimated Q_i.

[30] Composites of sea level pressure from the NCEPR were calculated for the 24 days in 1997 when the NCEPR most closely represents the mooring Q_i (Figure 10a) and the 23 days when the NCEPR most overestimates Q_i (Figure 10b). Similar patterns were obtained for 1996 and 1999 (not shown). The composites illustrate the tendency for NCEP to overestimate Q_i during periods of northwesterly winds. This analysis suggests that the NCEPR better reproduces cloudiness during organized synoptic disturbances and is less able to accurately reproduce low clouds and sea fog in fair weather conditions.

6. Summary and Discussion

[31] This study evaluates the quality of the NCEP/NCAR reanalysis using a series of buoy measurements in the Bering Sea and the NE Pacific. The main goal of this study is to provide information for investigators who use NCEPR in studies of the subpolar North Pacific (e.g., as input to physical and/or biological ocean models). Emphasis is placed on surface winds and shortwave radiation, as they are important parameters for forcing ocean models. Because the mooring data have not been assimilated into NCEPR, this analysis provides an independent measure of the quality of NCEPR output in these regions.

[32] NCEPR 10 m winds were well correlated at all of the moorings. However, the influence of topography very close to the coast is not well resolved by the NCEPR assimilation/model system and NCEPR winds near the coast should be used with caution. Although wind correlations are highly positive, a consistent bias of ~5% between NCEPR and the mooring wind speeds was found. It should be noted that wave shielding of the moorings during high wind conditions could result in wind speed measurements that underestimate the true wind speed [*Large et al.*, 1995]. However, this possibility was not evaluated in the context of this work.

[33] With one exception, after removing a seasonal cycle, correlation coefficients between downward shortwave radiation fluxes from NCEPR and from the data are significant but are not as high as the wind correlations. Correlation coefficients for the winter data at the OWS Papa location were the highest at 0.6. The summer data (with greater amplitude and variability) are correlated with coefficients greater than 0.36. Biases between NCEPR and the mooring data are consistently positive. NCEPR overestimates downward shortwave radiation by ~20 W m^{-2} at Papa and ~70–80 W m^{-2} in the Bering Sea. In the limited data evaluated here, there does not appear to be a seasonal dependence to the bias. The bias is likely due to underestimation of cloud coverage by the NCEPR. Analysis of wind patterns suggests that the NCEPR better reproduces cloudiness during organized synoptic disturbances and is less able to accurately reproduce low clouds and sea fog in fair weather conditions.

[34] On the basis of these results, NCEPR 10 m winds are well suited for forcing ocean models in the Bering Sea and Gulf of Alaska except when attempting to resolve processes within an internal deformation radius of the coast. On the other hand, we suggest that the NCEPR downward shortwave radiation should be reduced by ~70 W m^{-2} in the summer in the Bering Sea and ~20 W m^{-2} in the Papa region.

[35] **Acknowledgments.** We thank P. Stabeno for discussions and encouragement. D. Kachel prepared data products. W. Parker, C. DeWitt, and S. Salo helped deploy the moorings and prepare the instruments. NOPP (Papa) data were provided by the NOPP Program and the TAO Project Office. We thank P. Freitag and M. McPhaden for providing access to the NOPP data. We also thank the officers and crew of the NOAA ship *Miller Freeman*. Two anonymous reviewers contributed helpful suggestions. NCEP Reanalysis data were provided by the NOAA-CIRES Climate Diagnostics Center, Boulder, CO, USA, from their Web site at http://www.cdc.noaa.gov/. This work was performed while C. Ladd held a National Research Council Research Associateship Award at the NOAA

Pacific Marine Environmental Laboratory. This publication is supported by a grant to the Joint Institute for the Study of the Atmosphere and Ocean (JISAO) under NOAA Cooperative Agreement NA17RJ1232. This is PMEL contribution 2397 and JISAO contribution 905.

References

Bond, N. A., and J. M. Adams, Atmospheric forcing of the southeast Bering Sea Shelf during 1995–99 in the context of a 40-year historical record, *Deep Sea Res., Part II*, in press, 2002.

Bond, N. A., and P. J. Stabeno, Analysis of surface winds in Shelikof Strait, Alaska, using moored buoy observations, *Weather Forecast.*, *13*, 547–559, 1998.

Bony, S., Y. Sud, K. M. Lau, J. Susskind, and S. Saha, Comparison and satellite assessment of NASA/DAO and NCEP-NCAR reanalyses over tropical ocean: Atmospheric hydrology and radiation, *J. Clim.*, *10*, 1441–1462, 1997.

da Silva, A. M., C. C. Young, and S. Levitus, *Atlas of Surface Marine Data 1994, Volume 1, Algorithms and Procedures*, NOAA Atlas NESDIS 6, 51 pp., U.S. Dept. of Commerce, Washington, D.C., 1994.

Dorman, C. E., and D. W. Winant, Buoy observations of the atmosphere along the west coast of the United States, 1981–1990, *J. Geophys. Res.*, *100*, 16,029–16,044, 1995.

Flatau, M., L. Talley, and D. Musgrave, Interannual variability in the Gulf of Alaska during the 1991–94 El Niño, *J. Clim.*, *13*, 1664–1673, 2000.

Freitag, H. P., M. O'Haleck, G. C. Thomas, and M. J. McPhaden, Calibration procedures and instrumental accuracies for ATLAS wind measurements, *NOAA Tech. Memo. OAR PMEL-119*, 24 pp., 2001.

Hermann, A. J., P. J. Stabeno, D. B. Haidvogel, and D. L. Musgrave, A regional tidal/subtidal circulation model of the southeastern Bering Sea: Development, sensitivity analyses and hindcasting, *Deep Sea Res., Part II*, in press, 2002.

Kalnay, E., et al., The NCEP/NCAR 40-year reanalysis project, *Bull. Am. Meteorol. Soc.*, *77*(3), 437–472, 1996.

Kanamitsu, M., Description of the NMC global data assimilation and forecast system, *Weather Forecast.*, *4*, 335–342, 1989.

Kistler, R., et al., The NCEP-NCAR 50-year reanalysis: Monthly means CD-ROM and documentation, *Bull. Am. Meteorol. Soc.*, *82*(2), 247–268, 2001.

Klein, S. A., and D. L. Hartmann, The seasonal cycle of low stratiform clouds, *J. Clim.*, *6*, 1587–1606, 1993.

Kundu, P. K., Ekman veering observed near the ocean bottom, *J. Phys. Oceanogr.*, *6*, 238–242, 1976.

Lacis, A., and J. Hansen, A parameterization for the absorption of solar radiation in the Earth's atmosphere, *J. Atmos. Sci.*, *31*, 118–133, 1974.

Large, W. G., and S. Pond, Open ocean momentum flux measurements in moderate to strong winds, *J. Phys. Oceanogr.*, *11*, 324–336, 1981.

Large, W. G., J. Morzel, and G. B. Crawford, Accounting for surface wave distortion of the marine wind profile in low-level ocean storms wind measurements, *J. Phys. Oceanogr.*, *25*, 2959–2971, 1995.

National Research Council Committee on the Bering Sea Ecosystem, *The Bering Sea Ecosystem*, 320 pp., Natl. Acad. Press, Washington, D. C., 1996.

Norris, J. R., Low cloud type over the ocean from surface observations, part II, Geographical and seasonal variations, *J. Clim.*, *11*, 383–403, 1998.

Rossow, W. B., and R. A. Schiffer, ISCCP cloud data products, *Bull. Am. Meteorol. Soc.*, *72*(1), 2–20, 1991.

Scott, J. D., and M. A. Alexander, Net shortwave fluxes over the ocean, *J. Phys. Oceanogr.*, *29*, 3167–3174, 1999.

Shinoda, T., H. H. Hendon, and H. Glick, Intraseasonal surface fluxes in the tropical western Pacific and Indian Oceans from NCEP reanalyses, *Mon. Weather Rev.*, *127*, 678–693, 1999.

Smith, S. R., D. M. Legler, and K. V. Verzone, Quantifying uncertainties in NCEP reanalyses using high-quality research vessel observations, *J. Clim.*, *14*, 4062–4072, 2001.

Stabeno, P. J., J. D. Schumacher, R. F. Davis, and J. M. Napp, Under-ice observations of water column temperature, salinity and spring phytoplankton dynamics: Eastern Bering Sea shelf, *J. Mar. Res.*, *56*, 239–255, 1998.

Stanton, B. R., Ocean surface winds off the west coast of New Zealand: A comparison of ocean buoy, ECMWF model, and land-based data, *J. Atmos. Oceanic Technol.*, *15*, 1164–1170, 1998.

Wang, W., and M. J. McPhaden, What is the mean seasonal cycle of surface heat flux in the equatorial Pacific?, *J. Geophys. Res.*, *106*, 837–857, 2001.

Weare, B. C., Comparison of NCEP-NCAR cloud radiative forcing reanalyses with observations, *J. Clim.*, *10*, 2200–2209, 1997.

Yang, S.-K., Y.-T. Hou, A. J. Miller, and K. A. Campana, Evaluation of the Earth radiation budget in NCEP-NCAR reanalysis with ERBE, *J. Clim.*, *12*, 477–493, 1999.

N. A. Bond, Joint Institute for the Study of the Atmosphere and Ocean, University of Washington, Box 354235, Seattle, WA 98195-4235, USA. (bond@pmel.noaa.gov)

C. Ladd, Pacific Marine Environmental Laboratory, National Oceanic and Atmospheric Administration (NOAA), 7600 Sand Point Way NE, Seattle, WA 98115-6349, USA. (cladd@pmel.noaa.gov)